

 Open access • Journal Article • DOI:10.1021/JP0256948

Normal Vibrational Mode Analysis and Assignment of Benzimidazole by ab Initio and Density Functional Calculations and Polarized Infrared and Raman Spectroscopy

— [Source link](#) 

Mohamed A. Morsy, M.A. Alkhalidi, A. Suwaiyan





Institutions: King Fahd University of Petroleum and Minerals

Published on: 05 Sep 2002 - Journal of Physical Chemistry A (American Chemical Society)

Topics: Ab initio, Density functional theory and Raman spectroscopy

Related papers:

- [Heteroatom derivatives of indene: V. Vibrational spectra of benzimidazole](#)
- [Density-functional thermochemistry. III. The role of exact exchange](#)
- [Development of the Colle-Salvetti correlation-energy formula into a functional of the electron density](#)
- [FTIR and Raman studies on benzimidazole](#)
- [Vibrational spectroscopic investigations of \$m\(\text{benzimidazole}\)_2\text{Ni}\(\text{CN}\)_4\$ and \$\text{cd}\(\text{benzimidazole}\)\text{Cl}_2\$ complexes](#)

Share this paper:    

View more about this paper here: <https://typeset.io/papers/normal-vibrational-mode-analysis-and-assignment-of-40ao63y1wo>

Normal Vibrational Mode Analysis and Assignment of Benzimidazole by *ab Initio* and Density Functional Calculations and Polarized Infrared and Raman Spectroscopy

M. A. Morsy,^{*,†} M. A. Al-Khaldi,[‡] and A. Suwaiyan[†]

Department of Chemistry, King Fahd University of Petroleum & Minerals, Dhahran 31261, Saudi Arabia, and Department of Chemistry, Girls College, Dammam, Saudi Arabia

Received: February 27, 2002; In Final Form: July 8, 2002

Molecular structure and fundamental vibrational frequencies of benzimidazole (BZI) are reported using *ab initio*-Hartree–Fock (HF) and density functional theory (DFT) methods at different levels of calculation. Observed polarized IR and Raman fundamentals of polycrystalline, single crystal, KBr–BZI disks, and gaslike samples are analyzed and assigned by comparison to the computed values. The assignment of fundamentals shows a one-to-one correspondence between the observed and calculated fundamentals using the BLYP/6-31G* level of calculation without applying any scaling factor except for XH stretching (X represents C or N), where a 0.995 scaling factor has been used. Hydrogen bonding and its effects on some normal vibrational modes are discussed. The results show that the nonscaled BLYP/6-31G* level of calculation may be used as a reference for assessing the intermolecular hydrogen bonding effect.

Introduction

Benzimidazole (BZI) and a series of substituted BZI analogues are fundamental compounds of many important chemicals: pharmaceutical fine chemicals,^{1–7} polymers,^{8–11} and corrosion inhibitors.^{12–15} These different applications have attracted many experimentalists and theorists to investigate the spectroscopic properties of benzimidazole^{15–20} and some of its derivatives.^{21–23}

Several vibrational studies of BZI were performed on its KBr disk,¹⁸ solid and solution,²⁴ KBr mull,¹⁹ melt and single crystal,¹⁷ and its gaslike phase in the Ar matrix²⁵ to settle its modes' assignments. However, there is still some ambiguity in the assignment of certain fundamental modes due to their low intensities or extensive band overlapping. The earlier polarized IR and Raman results¹⁷ resolved some of these ambiguities, but a reliable theoretical study in conjunction with these results is required to shed more light on the analysis and assignment of the fundamentals. The successful use of *ab initio* Hartree–Fock (HF) computational method in our analysis of the vibrational modes of 5-methoxyindole,²⁶ conformer stabilities' determination of thymine,²⁷ and a liquid crystalline system²⁸ motivated us to advance our earlier analysis of the polarized IR and Raman results¹⁷ of benzimidazole.

In this study, we compare the predictive abilities of different theoretical methods using various basis sets in reproducing the experimental molecular geometry and vibrational results. The calculations of molecular structure and normal vibrational mode analyses of BZI were performed at Hartree–Fock (HF) and two density functional theory (DFT) methods, namely, Becke–Lee–Yang–Parr (BLYP) and Becke 3–Lee–Yang–Parr (B3LYP), using the 3-21G and 6-31G* basis sets. The results confirm that DFT with a specific basis set is sufficiently powerful to predict fundamentals even without using any scaling factor

except for XH stretching modes, where a 0.995 scaling factor was used. Moreover, the thorough analysis of the reported^{17,25} polarized Raman spectra from a single crystal of BZI and its well-resolved FT-IR spectra of the gaslike state and of KBr disks rationalized the effect of the intermolecular hydrogen bonding on some fundamental modes.

Experimental Section

Benzimidazole (BZI) was obtained from Fluka and was used after repeated crystallization from an ethanol–water mixture to remove particulate and colored impurities. IR spectra of a series of BZI–KBr disks were recorded at room temperature on a Perkin-Elmer 16PC FT-IR spectrometer at 2 cm⁻¹ resolution. Vibrational spectra in Figures 1 and 2 show that the extensive band overlapping in the IR and broadening problems could be overcome by the proper procedure of dilution, grinding, and preparation of BZI–KBr disks. This procedure has produced clear IR spectra (e.g., spectra C and D of Figures 1 and 2), which exhibited a one-to-one correspondence of fundamentals with the Raman spectrum (spectrum F in both Figures) of the polycrystalline BZI.¹⁷ These reported IR spectra have also comparable band features to IR spectra of BZI in the gaslike state (spectrum E in both Figures).²⁵

Polarized IR and Raman spectra of polycrystalline BZI and polarized Raman spectra of a large single crystal of BZI were reported in our earlier study.¹⁷ The high-resolution polarized Raman spectra from a single crystal of BZI has been used to identify some of the poorly resolved or weakly represented fundamentals from the Raman spectrum of polycrystalline BZI in the 100–1700 cm⁻¹ range (Figure 1S).

Method of Calculations

Calculations on BZI were performed at the LCAO-MO-SCF restricted Hartree–Fock (HF) and density functional theory (DFT) levels using Becke–Lee–Yang–Parr (BLYP) and Becke's nonlocal three-parameter exchange and correlated functional with Lee–Yang–Parr correlation (B3LYP) func-

* To whom all correspondence should be addressed. E-mail: mamorsy@kfupm.edu.sa.

[†] King Fahd University of Petroleum & Minerals.

[‡] Girls College.

Figure 1. Vibrational spectra of benzimidazole: (A–D) FT-IR of polycrystalline samples at different concentration from high to low, respectively. (E) FT-IR of gaslike sample trapped in argon matrix. (F) Raman of polycrystalline sample. Expansion notation (e.g., $\times 3$) has to be applied to the adjacent vibrational band on the left to get the original intensity.

tional methods. The runs were executed on a relatively fast personal computer. The optimized molecular geometry of BZI was obtained without any structural constraint on the planarity using the most common basis sets, namely 3-21G* and 6-31G*, with the GAUSSIAN 98W program.²⁹ A planar geometry was found to be the most stable one. In addition to the reported³⁰ X-ray molecular parameters of BZI, all the estimated bond lengths and angles of the optimized BZI molecule are listed in Table 1.

As expected, the computed fundamental frequencies using HF/3-21G* and HF/6-31G* were overestimated by about 10–12%.³¹ It, therefore, has been advisable to scale their computed values by a single uniform factor of 0.91^{32–35} or 0.8929.³⁶ However, other results on planar molecules indicated^{26,37} that two scaling factors of 0.9017 for in-plane modes and 0.8383 for out-of-plane modes could be used to bring closer the calculated and observed frequencies. On the other hand, computational results on fundamentals using DFT methods showed that these methods reproduce experimental vibrational frequencies with higher accuracy than do the HF and MP2 methods.^{37–44} For example, results on predicting the fundamentals of 20 small molecules (e.g., benzene, ether, etc., whose vibrational spectra are exactly assigned) by Rauhut and Pulay⁴² using BLYP and B3LYP functional methods derived uniform scaling factors of 0.995 and 0.963, respectively.

In our analysis, the HF-computed BZI vibrational modes have been scaled with the proposed^{26,37} scaling factors of the planar system. For DFT-computed fundamentals, the proposed⁴² scaling factor of 0.963 was very suitable for scaling at the B3LYP level of calculations, whereas no scaling factor was required for

Figure 2. XH stretching vibrational spectra of benzimidazole: (A–D) FT-IR of polycrystalline samples at different concentration from high to low, respectively. (E) FT-IR of gaslike sample trapped in argon matrix. (F) Raman of polycrystalline sample. Expansion notation (e.g., $\times 3$) has to be applied to the adjacent vibrational band on the left to get the original intensity.

BLYP-computed fundamentals except for the X–H stretching modes where the 0.995 scaling factor was implemented.

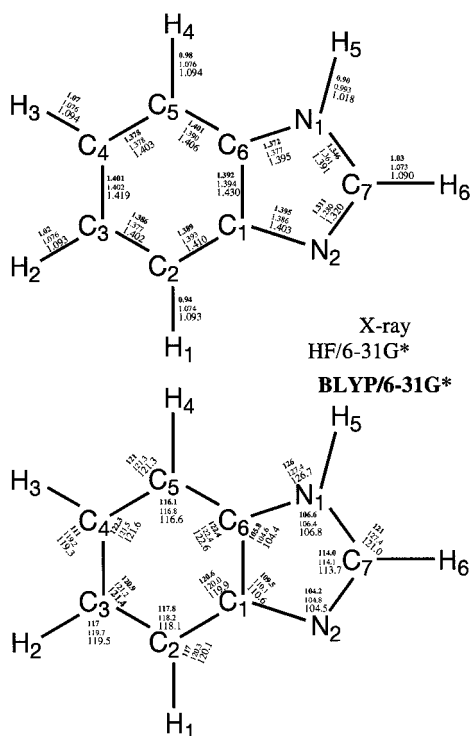
HyperChem⁴⁵ under MS-Windows has been used to display all the vibrational modes associated with each calculated spectral line. The computed IR spectrum has been produced from Gaussian output files by FreqChk utilities⁴⁶ in the GAUSSIAN 98W package. The HyperChem vibrational spectrum with active IR vector rendering has been used to graphically display the normal modes associated with individual vibrations. For the sake of an informative graphical display, representative IR vectors, which have strengths of 20% or higher, have been displayed for all the BZI-fundamentals.

Results and Discussion

Geometric Structure. Molecular geometry and numbering of atoms of benzimidazole (BZI) are depicted in Figure 3, which also shows some of the estimated structure parameters and experimental bond lengths and bond angles. Although it is well-known that the HF method underestimates bond lengths,³⁶ the HF/6-31G* method of calculation has the least bond length discrepancy (less than 0.01 Å) relative to the X-ray values (Figure 4A). On the other hand, the BLYP/3-21G* method of calculation gives the largest discrepancy with X-ray values. Closer examination of the bond lengths in Figure 4A estimated using HF/6-31G* relative to the X-ray values shows that large deviations are observed in the bond lengths of C5–C6, N1–C7, and C7–N2. Bonds C5–C6 and C7–N2 are stretched whereas N1–C7 is shortened. These deviations may be attributed to the solid state intermolecular interactions, particularly

TABLE 1: Optimized and X-ray Geometrical Parameters of BZI, Lengths in Ångstroms and Angles in Degrees

parameters ^a	HF		BLYP		B3LYP		
	X-ray	3-21G*	6-31G*	3-21G*	6-31G*	3-21G*	6-31G*
A. Bond Length							
C ₁ –C ₂	1.389	1.38561	1.39255	1.40696	1.40957	1.3969	1.40044
C ₂ –C ₃	1.386	1.37563	1.37697	1.40248	1.40226	1.3913	1.39084
C ₃ –C ₄	1.401	1.40117	1.4024	1.42058	1.41921	1.41084	1.41012
C ₄ –C ₅	1.378	1.37723	1.37815	1.40426	1.40334	1.3923	1.39204
C ₅ –C ₆	1.401	1.38685	1.39002	1.40519	1.40568	1.39491	1.39622
C ₆ –C ₁	1.392	1.39697	1.39403	1.43619	1.42985	1.421141	1.41642
C ₆ –N ₁	1.372	1.38244	1.37662	1.40191	1.39544	1.39176	1.38473
N ₁ –C ₇	1.346	1.381	1.36108	1.41	1.391	1.395	1.378
C ₇ –N ₂	1.311	1.29092	1.27999	1.33448	1.32034	1.31993	1.30656
N ₂ –C ₁	1.395	1.40322	1.38561	1.42259	1.40333	1.41066	1.39106
C ₂ –H ₁	0.94	1.0702	1.07442	1.08883	1.09338	1.08162	1.086
C ₃ –H ₂	1.02	1.0719	1.07579	1.09094	1.09346	1.08301	1.08639
C ₄ –H ₃	1.07	1.0714	1.07567	1.09118	1.09452	1.08312	1.08708
C ₅ –H ₄	0.98	1.0712	1.07569	1.09106	1.09421	1.08353	1.08704
N ₁ –H ₅	0.9	0.9943	0.993453	1.02121	1.01847	1.01242	1.00924
C ₇ –H ₆	1.03	1.0644	1.07263	1.08443	1.09004	1.07709	1.08336
B. Bond Angle							
C ₁ C ₂ C ₃	117.8	118.2	118	118.4	118.1	118.3	118.1
C ₂ C ₃ C ₄	120.9	120.9	121.2	121.2	121.4	121.1	121.4
C ₃ C ₄ C ₅	122.3	121.5	121.5	121.5	121.6	121.4	121.6
C ₄ C ₅ C ₆	116.1	117.2	116.8	117.2	116.6	117.3	116.7
C ₅ C ₆ C ₁	122.4	121.7	122.4	121.9	122.6	121.8	122.6
C ₆ C ₁ C ₂	120.6	120.4	120	119.9	119.7	120	119.7
C ₁ C ₆ N ₁	105.8	105.3	104.6	104.9	104.4	105	104.4
C ₆ N ₁ C ₇	106.6	106.7	106.4	107.1	106.8	107.1	106.7
N ₁ C ₇ N ₂	114	112.7	114.1	112.9	113.7	112.8	113.7
C ₇ N ₂ C ₁	104.2	105.9	104.8	104.9	104.5	105.2	104.6
N ₂ C ₁ C ₆	109.5	109.3	110.1	110.2	110.6	109.9	110.5
C ₁ C ₂ H ₁	117	119.9	120.3	119.8	120.1	119.9	120.2
C ₂ C ₃ H ₂	117	119.9	119.7	119.7	119.5	119.7	119.6
C ₃ C ₄ H ₃	111	119.2	119.2	119.3	119.3	119.2	119.3
C ₄ C ₅ H ₄	121	121.1	121.3	120.8	121.3	120.8	121.3
C ₆ N ₁ H ₅	126	126.8	127.4	126.2	126.7	126.4	126.9
N ₁ C ₇ H ₆	121	121.7	121	121.5	121	121.6	121.1

**Figure 3.** Observed and selected values of the calculated structural parameters of benzimidazole molecule.

the reported strong hydrogen bonding,³⁰ which is 2.0 Å long from H₅ to N₂.

Regarding the C–H and N–H bond lengths, it is well-known³⁶ that due to low scattering factors of hydrogen atoms in X-ray diffraction, the experimental bond lengths of X–H bonds are much shorter than the estimated bond lengths.^{27,36} As expected, Figure 4B shows that most of the observed C–H bond lengths of BZI are shorter than the estimated values. Exceptions for this trend are observed in C₄–H₃ and N₁–H₅ bond lengths that are remarkably stretched out to approach the estimated values. The prolonged N₁–H₅ bond length of the imidazole (Im) ring can be linked to the intermolecular hydrogen bonds.^{47–49} However, the stretch of the C₄–H₃ bond length of the benzene (Bz) ring may be attributed to crystal packing effects.

The estimated bond angles (Figure 5) agree very well with the observed X-ray values. Discrepancies are about 0.9° for bond angles except for some of the Bz–CCH angles. The largest discrepancy of about 8° is observed in the C₃C₄H₃ bond angle. This deviation may be attributed to a crystal packing effect, namely, molecular structure strain between benzene parts of different BZI molecules (see molecules III and VI in the unit cell presentation in Figure 6),¹⁷ which is further evidence of the elongation in the C₄–H₃ bond length.

Fundamental Modes. Benzimidazole has a C_s symmetry and 39 fundamental modes; all of them are IR and Raman active. These modes include 12-depolarized out-of-plane modes with A'' symmetry and 27-polarized in-plane modes with A' symmetry. Tables 1S, 2S, and 3S (Supporting Information) present a comprehensive summary of all fundamentals. These tables show the reported fundamentals of BZI and their assignments from IR spectra of KBr disks,¹⁹ partially oriented solid,¹⁷ a

Figure 4. Observed and calculated bond lengths of benzimidazole: (A) C–C and C–N bond lengths; (B) C–H and N–H bond lengths.

gaslike phase trapped in an argon matrix,²⁵ and observed IR values from the highly resolved absorption spectra C and D of Figures 1 and 2. Estimated values of all the fundamentals, their scaled values, intensities, and the corresponding IR vector graphical representation for the optimized geometries of single BZI molecule at each *ab initio* level used in this study are also included in Tables 1S, 2S, and 3S. The observed fundamental frequencies and their best estimated values and mode assignments have been extracted from these tables and are presented in Table 2.

The polarization of the incident and scattered light has enormous effects on the intensities of vibrational modes (Figure 1S). The BZI fundamentals from these polarized spectra and Raman spectrum of BZI powder are also included in Tables 1S and 2S. A close examination of these reported polarized Raman spectra indicates that many vibrations become weaker or even disappear as a result of the change in polarization, except for *bb*- and *cc*-polarized Raman spectra. These two spectra show the clearest identified BZI fundamentals compared to the powder sample. This is in agreement with the reported results on the

oriented gas model,¹⁷ which predicts the vibrations with *A'* symmetry will be most intense parallel to the *b*-axis whereas *A''* types vibrations will be most intense parallel to the *c*-axis.

Out-of-Plane Modes. Systematic comparison of the observed out-of-plane fundamentals of solid samples with the corresponding fundamentals of the gaslike sample (Table 2 and Figure 1) shows different correlations. For the 626 and 887 cm^{-1} modes, the frequency deviations, which are quite large, are about 180 and 30 cm^{-1} , respectively. On the other hand, the correlation is quite good for the 424, 578, 635, 746, 752, 902, and 933 cm^{-1} , modes with an average deviation of about 6 cm^{-1} . This small deviation may indicate that these well-predicted modes exhibit no or minimal hydrogen bonding and/or crystal packing effects. Therefore, they can be considered as appropriate fundamentals among the out-of-planes modes to compare with the computed values.

A check of the computed values listed in Table 1S relative to the above-mentioned modes shows that the closest estimating of these fundamentals are obtained by the BLYP/6-31G* level of calculation without applying the scaling factor. This agree-

Figure 5. Observed and calculated bond angles of benzimidazole: (A) C–C–C and C–C–N bond lengths; (B) C–C–H and C–N–H bond lengths.

ment is manifested in the marginally lowest mean frequency deviation (mfd), $|\nu^{\text{exp}} - \nu^{\text{theor}}|$, of about 6 cm^{-1} relative to the observed modes of the solid samples and about 10.5 cm^{-1} relative to the gaslike sample. The other levels of calculation, even the HF/6-31G* one, which give the best estimates of bond lengths (Figure 4A), have a much higher mfd. Some of these levels of calculation improved upon applying the recommended^{26,37,42} scaling factors to them. For example, the scaled HF/6-31G* gives a mfd value of about 32 cm^{-1} , whereas the nonscaled one gives a mfd value of about 40 cm^{-1} . On the other hand, the observed low mfd between the observed out-of-plane modes of BZI and their computed values using BLYP/6-31G* causes us to limit the comparison of the remaining out-of-plane modes to the estimated results from this level of calculation (Table 2).

For the 626 cm^{-1} mode of vibration, the largest frequency deviation (fd) occurs relative to the gaslike sample (fd = 177 cm^{-1}) as well as to the estimated one using the BLYP/6-31G* level of calculation (fd = 220 cm^{-1}). This large fd value is expected because this mode is attributed to NH out-of-plane bending¹⁹ and this NH is a hydrogen bonding donor site in BZI molecule (Figure 6). Moreover, comparison between its ob-

served value in the gaslike sample and the corresponding calculated value shows a difference of about 40 cm^{-1} . This difference may be attributed to the presence of the intermolecular hydrogen bonding of BZI molecules in the argon matrix. The results also indicate that the hydrogen bond effect is much weaker in the argon matrix than in the solid samples.

The second largest fd value is observed for the 887 cm^{-1} band, which has a deviation of about 29 cm^{-1} relative to the gaslike sample and 57 cm^{-1} for the crystalline material relative to the estimated value. The IR vector representation for this mode in Table 1S and its summarized assignment in Table 2 show a large contribution of the Bz-CH wags. Therefore, this frequency deviation could be attributed to crystal packing and/or the molecular aggregation. This deviation also correlates with the observed distortions in the CH bond lengths and CCH bond angles of the benzene part as discussed above.

Modes 242 , 270 , and 847 cm^{-1} observed in this region have no corresponding modes from the gaslike sample. However, all of them show remarkable frequency deviations for crystalline samples relative to their estimated values (24 , 22 , and 50 cm^{-1} , respectively). According to the reported¹⁹ assignment, namely, imidazole-CH (Im-CH) bending of the 847 fundamental and

TABLE 2: Observed and Estimated Frequencies (cm⁻¹), Relative Intensities, and Assignments of the Fundamental Modes of Benzimidazole^a

solid IR ^b	solid Ram ^c	gaslike ^d	estimated frequencies ^e	assignments/symmetry ^f
Out-of-Plane Modes				
242 (m)	247 (w)		218 (6.66)	Bz & Im CH wags (sym)/A''
270 (m)	272 (vw)		248 (1.65)	Bz & Im CH wags (asym)/A''
626 (m)	625 (m)	449 (vs)	406 (99.94)	NH wag/A''
424 (s)	424 (w)	425 (s)	421 (2.11)	mainly C2H, C5H, and Im NH wags/A''
578 (w)	580 (w)	586 (w)	570 (4.36)	mainly C3H, C4H, and NH wags/A''
635 (m)	636 (m)	647 (w)	630 (2.11)	mainly Im CH & NH wags (asym)/A''
746 (vs)	746 (w)	743 (vs)	731 (45.57)	Bz CH's wags (sym)/A''
752 (vs)	755 (w)	766 (m)	750 (3.80)	mainly Bz CH's wags (asym)/A''
847 (w)	848 (w)		797 (8.79)	Im CH wag/A''
887 (m)	890 (w)	860 (m)	830 (1.85)	Bz CH's and Im CH wags/A''
902 (w)	905 (vw)	903 (m)	890 (1.79)	mainly C2H, C3H, and C5H wags/A''
933 (w)	934 (w)	931 (w)	933 (0.06)	Bz CH's wags (asym)/A''
In-Plane Modes				
419 (s)	418 (w)	417 (m)	405 (7.05)	Bz and Im rings bending/A'
542 (w)	544 (m)	538 (vw)	537 (0.15)	Bz and Im rings stretching/A'
618 (m)	617 (m)	621 (vw)	610 (0.05)	bending & bond stretching (asym)/A'
768 (s)	778 (vs)	780 (m)	767 (3.89)	angle bending & bond stretching (sym)/A'
876 (m)	881 (w)	877 (m)	863 (3.39)	mainly C2H, C5H, and C7H bending/A'
958 (s)	958 (w)	947 (s)	912 (1.85)	mainly C2H and NH bending/A'
1005 (m)	1004 (vs)	1011 (m)	1005 (3.14)	Bz CH's bending (sym)/A'
1134 (s)	1135 (s)	1082 (s)	1061 (14.89)	Im CH and NH bending/A'
1112 (w)	1110 (m)	1115 (w)	1103 (1.24)	Bz CH's and Im CH bending/A'
1158 (w)	1163 (vw)	1163 (vw)	1151 (2.57)	Bz CH's bending (asym)/A'
1202 (m)	1204 (w)	1199 (w)	1170 (1.23)	Im XH's, C2H, C3H, and C5H bending (asym)/A'
1246 (vs)	1250 (m)	1254 (vs)	1241 (22.07)	Im XH's, C3H, and C4H bending (sym)/A'
1274 (vs)	1277 (vs)	1264 (vs)	1253 (26.83)	Im XH's, C2H, C3H, and C5H bending (sym)/A'
1300 (s)	1304 (m)	1306 (m)	1299 (5.11)	Bz CH's and Im CH bending/A'
1345 (w)	1345 (m)	1346 (m)	1349 (36.89)	Im XH's, C2H, and C3H bending (sym)/A'
1410 (vs)	1412 (s)	1394 (vs)	1390 (9.66)	Im XH's, C2H, C4H, and C5H bending (asym)/A'
1459 (w)	1463 (w)	1458 (s)	1445 (22.44)	Bz CH's and Im XH's bending (sym)/A'
1478 (s)	1480 (m)	1494 (sh)	1478 (12.70)	Bz CH's and C7H bending and N2C7 St/A'
1494 (m)	1498 (m)	1503 (vs)	1491 (8.50)	Bz CH's and Im XH's bending (asym)/A'
1588 (m)	1590 (s)	1593 (w)	1576 (2.93)	C4H and NH bending and Bz CC's St/A'
1620 (w)	1623 (w)	1621 (vw)	1613 (6.29)	Bz and Im XH's bending and CC's St/A'
XH Stretching Modes				
3062 (w)		3066 (w)	3098 [3083] (0.16)	Bz C3H, C4H, and C5H stretching (asym)/A'
2926 (m)	2930 (w)	3088 (m)	3108 [3092] (18.01)	Bz C3H and C5H stretching/A'
3094 (w)	3091 (w)	3095 (sh)	3120 [3104] (33.70)	Bz C3H, C4H, and C5H stretching (sym)/A'
3115 (m)	3112 (m)	3114 (w)	3131 [3115] (17.57)	Bz C2H, C3H, and C4H stretching/A'
3038 (w)	3021 (sh)	3145 (w)	3172 [3156] (5.62)	Im CH stretching/A'
3423 (b)	3055 (vs)	3509 (vs)	3532 [3514] (30.74)	Im NH stretching/A'

^a Abbreviations: vs, very strong; s, strong; m, medium; w, weak; vw, very weak; sh, shoulder; f, fundamental; A', symmetry; p, polarized; sym, symmetrical; asym, asymmetric. ^b IR of KBr disks. ^c Raman of powder. ^d FT-IR of gaslike BZI in Ar matrix. ^e Estimated vibrational modes using BLYP/6-31G* [its scaled value] (its intensity in km/mol). ^f Summary of the estimated graphical representation/estimated mode symmetry.

its estimated mode assignment in Table 2, the large fd value is expected because of the hydrogen bonding effect in the Im ring. The IR vector representation for the other modes (242 and 270 fundamentals) may relate the observed fd values to combined effects of hydrogen bonding and the crystal packing factors in BZI intermolecular system.

In-Plane Modes. Table 2S includes in-plane vibrational modes other than CH and NH stretching. These modes have been observed and located within the IR spectral range 100–1700 cm⁻¹. The summary of the assignment of these modes from Figures 1 and 1S and the calculated values in Table 2 shows that these fundamentals also have different correlations between the solid and the gaslike samples. This different correlation is much clearer between the observed and estimated values using BLYP/6-31G* level of calculation.

Comparison between the observed in-plane modes summarized in Table 2 and the calculated fundamentals using BLYP/6-31G* level of calculation shows good agreement in 16 modes. The mfd values of solid versus calculated and gaslike versus calculated frequencies are 6.4 and 11 cm⁻¹, respectively. On the other hand, the rest of the in-plane modes, namely 958, 1134,

1202, 1274, and 1410 cm⁻¹ give large fd values. The values of these deviations are as follows: 46, 73, 32, 21, and 20 cm⁻¹, respectively.

The observed largest fd values for the 958 and 1134 cm⁻¹ modes are expected because they are related to the hydrogen bonding site in the BZI molecule. This is in good agreement with the assignment of these modes as Im-ring in-plane and NH in-plane vibrational bending,¹⁹ respectively. Moreover, comparison of the observed frequencies of these modes in the gaslike state and the corresponding calculated values shows a difference of about 35 and 21 cm⁻¹, respectively. These deviations are further evidence of the presence of the intermolecular hydrogen bonding of BZI molecules in the argon matrix but with a much weaker effect than the solid samples.

Smaller fd values observed in the case of modes 1202, 1274, and 1410 cm⁻¹ may indicate that they are related to the same effect. All of them have been assigned as benzene-CH (Bz-CH) in-plane bends.¹⁹ Therefore, these deviations may be further evidence of the effect of crystal packing and/or the molecular aggregation. They also confirm the observed distortions in the

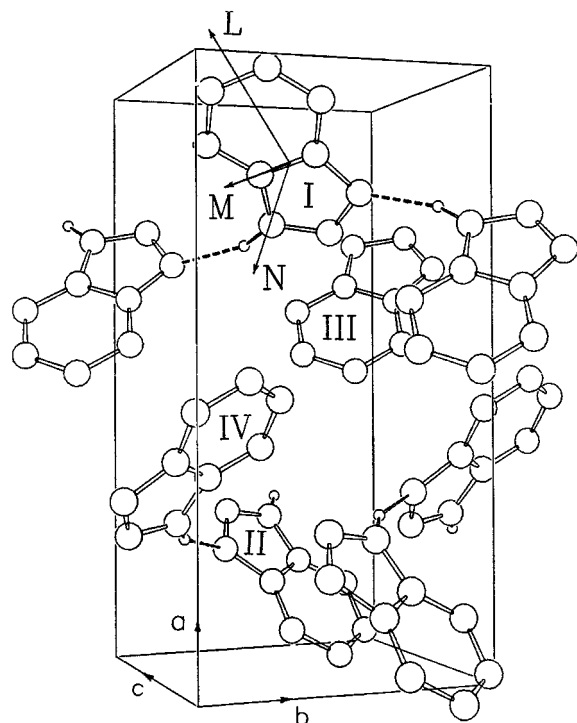


Figure 6. Benzimidazole unit cell with molecular axis frame (L, M, N).

CH bond lengths and CCH bond angles of the benzene part, as discussed above.

The summary of the in-plane results in Table 2S validates the earlier observation on the different level of calculations. The nonscaled BLYP/6-31G* level of calculation shows the smallest mfd values relative to the other levels. The mfd values of the solid and gaslike cases relative to the calculated fundamentals (about 6 and 11 cm^{-1} , respectively) are the same for both out-of-plane and in-plane modes.

XH Stretching Modes. The observed spectra of these vibrational modes in solid and gaslike states are presented in Figure 2. Bands due to these modes have very different features from spectrum A down to spectrum D. For example, extensive band broadening and overlapping takes place in spectrum A that is gradually reduced by dilution until the most resolved one in spectrum D. This effect may be correlated with strong solute–solute interaction between BZI molecules. The weakness of this interaction is confirmed by the observation of band resolution in spectra C and D in Figures 1 and 2. It is also observed that the dilution process intensifies a broad IR band at about 3423 cm^{-1} . This band may be correlated with the NH stretching vibration, and its broadening is related to the intermolecular hydrogen bonding effect. The summary in Table 2 shows the fd values of the 3423 cm^{-1} mode relative to the gaslike sample (about 91 cm^{-1}) and to the calculated fundamentals (about 109 cm^{-1}). These deviations confirm the relation between this mode and the intermolecular hydrogen bonding effect. The broadening properties of this mode may indicate that the hydrogen bonding is not the only intermolecular solute–solute interaction factor that is responsible for the observed extensive band broadness in spectrum A of Figure 2. Thus, the extensive broadening in spectrum A may be related to a strong intermolecular aggregation within the solid state of the BZI system.

The listed summary in Table 2 under the XH stretching modes section indicates that the other solid-state fundamentals are related to CH stretching vibrational modes. Comparison between

the values of these modes and their gaslike values indicates that the 2926 and 3038 cm^{-1} modes show very high fd values of about 162 and 107 cm^{-1} , respectively. Mode 3038 cm^{-1} is assigned as Im-CH stretching vibrations and 2926 cm^{-1} is a Bz-CH stretching vibration. The deviation of these modes can be related to the hydrogen bond effect that takes place at the Im ring site. For 2926 cm^{-1} mode, the observed deviation is most probably related to the crystal packing and/or the molecular aggregation because it is assigned as a Bz-CH's stretching vibration. This deviation is further evidence of distortions in the CH bond lengths and CCH bond angles of benzene part.

On the other hand, for the solid and gaslike phases the frequencies 3062, 3094, and 3115 cm^{-1} are in very good agreement if not identical. These modes have an mfd value relative to the BLYP/6-31G* calculated values equal to 28 cm^{-1} that is improved to about 5.7 cm^{-1} after applying the reported⁴² scaling factor 0.995. The application of the scaling factor on the calculated XH stretching modes makes the BLYP/6-31G* level of calculation again the best level of calculation among these investigated.

Conclusion

The experimental results obtained in this and previous studies of the BZI system compared to its theoretical data allowed us to derive correlations between the observed frequency deviations of certain modes and hydrogen bonding interaction or other molecule–molecule interactions. The study shows different trends in the calculated bond length and bond angle discrepancies from the X-ray parameters. The CH bond lengths and CCH bond angles are found to be very sensitive to these correlations. Moreover, the predicted vibrations show that DFT methods reproduce experimental vibrational frequencies with higher accuracy than do the HF calculations, a result in good agreement with the previous studies.⁴² The computed values also indicate that the nonscaled BLYP/6-31G* level of calculation gives the best estimates of fundamentals compared to both solid and/or gaslike samples, including the lowest mfd values except for the XH stretching modes, which need to be scaled with a scaling factor of 0.995. Finally, the study indicates that the nonscaled BLYP/6-31G* level of calculation may be used as reference values for identifying the intermolecular hydrogen bonding effect and any other molecule–molecule interactions.

Acknowledgment. We gratefully acknowledge the support of King Fahd University of Petroleum and Minerals.

Supporting Information Available: Figure 1S represents the high-resolution polarized Raman spectra from a single crystal of BZI compared to Raman spectrum of polycrystalline BZI in the 100–1700 cm^{-1} range. Tables 1S, 2S, and 3S present a comprehensive summary of the observed fundamental frequencies of benzimidazole. They also include the estimated values of these fundamentals, their scaled values, intensities, and the corresponding IR-vector graphical representation for the optimized geometries of single BZI molecule at each ab initio level used in this study. These materials are available free of charge via the Internet at <http://pubs.acs.org>.

References and Notes

- (1) White, A. W.; Almasy, R.; Calvert, A. H.; Curtin, N. J.; Griffin, R. J.; Hostomsky, Z.; Maegley, K.; Newell, D. R.; Srinivasan, S.; Golding, B. T. *J. Med. Chem.* **2000**, *43*, 4084–4097.
- (2) Chen, J. J.; Wei, Y.; Drach, J. C.; Townsend, L. B. *J. Med. Chem.* **2000**, *43*, 2449–2456.

- (3) Tapia, I.; Alonso-Cires, L.; López-Tudanca, P. L.; Mosquera, R.; Labeaga, L.; Innerarity, A.; Orjales, A. *J. Med. Chem.* **1999**, *42*, 2870–2880.
- (4) Sjöström, J. *J. Med. Chem.* **1998**, *41*, 1777–1788.
- (5) Townsend, L. B. *J. Med. Chem.* **1998**, *41*, 1252–1262.
- (6) Tang, J. C. *J. Med. Chem.* **1997**, *40*, 3937–3946.
- (7) Wilson, W. D. *J. Med. Chem.* **1996**, *39*, 1452–1462.
- (8) Carrière, F. *Chem. Mater.* **1997**, *9*, 1989–1993.
- (9) Yamamoto, T. *Macromolecules* **1998**, *31*, 6063–6070.
- (10) Hedrick, J. L. *Macromolecules* **1996**, *29*, 7335–7341.
- (11) Brown, G. P.; Aftergut, S. *J. Polym. Sci., Part A* **1964**, *2*, 1839.
- (12) Christov, M. *Langmuir* **1996**, *12*, 2083–2089 and references therein.
- (13) Tompkins, H. G.; Sharma, S. P. *Surf. Interface Anal.* **1982**, *4*, 261.
- (14) Hobbins, N. D.; Roberts, R. F. *Surf. Technol.* **1979**, *9*, 235.
- (15) Thibault, S. *Corros. Sci.* **1977**, *17*, 701.
- (16) Mohan, S.; Sundaragan, J.; Mink, J. *Thermochim. Acta A* **1991**, *47*, 1111.
- (17) Suwaiyan, A.; Zwarich, R.; Baig, N. *J. Raman Spectrosc.* **1990**, *21*, 243.
- (18) Tompkins, H. G.; Allara, D. L.; Pasteur, G. A. *Surf. Interface Anal.* **1983**, *5*, 101–104.
- (19) Cordes, M. M.; Walter, J. L. *Spectrochim. Acta* **1968**, *24*, 1421.
- (20) Varsanyi, G. *Assignments for Vibrational Spectra of Seven Hundred Benzene Derivatives*; John Wiley & Sons: New York, 1974; Vol. 1.
- (21) Santra, S.; Krishnamoorthy, G.; Dogra, S. K. *J. Phys. Chem. A* **2000**, *104*, 476–482.
- (22) Luque, F. J. *J. Phys. Chem. A* **1999**, *103*, 4525–4532.
- (23) Warner, I. M. *J. Phys. Chem. A* **1997**, *101*, 5296–5301.
- (24) Borach, B.; Wood, J. L. *Can. J. Chem.* **1976**, *54*, 2470.
- (25) Schoone, K.; Smets, J.; Houben, L.; Van Bael, M. K.; Adamowicz, L.; Maes, G. *J. Phys. Chem. B* **1998**, *102*, 4863.
- (26) Suwaiyan, A.; Morsy, M. A. *Spectrochim. Acta Part A* **1997**, *53*, 575–588.
- (27) Morsy, M. A.; Al-Somali, A. M.; Suwaiyan, A. *J. Phys. Chem. B* **1999**, *103*, 11205–11210.
- (28) Morsy, M. A.; Oweimreen, G. A.; Al-Tawfig, A. M. *J. Phys. Chem. B* **1998**, *102*, 3684–3691.
- (29) Frisch, M. J.; Trucks, G. W.; Schlegel, H. B.; Scuseria, G. E.; Robb, M. A.; Cheeseman, J. R.; Zakrzewski, V. G.; Montgomery, J. A., Jr.; Stratmann, R. E.; Burant, J. C.; Dapprich, S.; Millam, J. M.; Daniels, A. D.; Kudin, K. N.; Strain, M. C.; Farkas, O.; Tomasi, J.; Barone, V.; Cossi, M.; Cammi, R.; Mennucci, B.; Pomelli, C.; Adamo, C.; Clifford, S.; Ochterski, J.; Petersson, G. A.; Ayala, P. Y.; Cui, Q.; Morokuma, K.; Malick, D. K.; Rabuck, A. D.; Raghavachari, K.; Foresman, J. B.; Cioslowski, J.; Ortiz, J. V.; Stefanov, B. B.; Liu, G.; Liashenko, A.; Piskorz, P.; Komaromi, I.; Gomperts, R.; Martin, R. L.; Fox, D. J.; Keith, T.; Al-Laham, M. A.; Peng, C. Y.; Nanayakkara, A.; Gonzalez, C.; Challacombe, M.; Gill, P. M. W.; Johnson, B. G.; Chen, W.; Wong, M. W.; Andres, J. L.; Head-Gordon, M.; Replogle, E. S.; Pople, J. A. *Gaussian 98*, revision A.7; Gaussian, Inc.: Pittsburgh, PA, 1998.
- (30) Dik-Edixhoven, C. J.; Schent, H.; van der Meer, H. *Cryst. Struct. Commun.* **1973**, *2*, 1647.
- (31) Foresman, J. B.; Frisch, A. *Exploring Chemistry with Electronic Structure Methods: A Guide to Using Gaussian*; Gaussian: Pittsburgh, PA, 1996.
- (32) Pongor, G.; Fogarasi, G.; Boggs, J. E. *J. Mol. Spectrosc.* **1985**, *114*, 445.
- (33) Pongor, G.; Fogarasi, G.; Boggs, J. E. *J. Am. Chem. Soc.* **1985**, *107*, 6487.
- (34) Xie, Y.; Fan, K.; Boggs, J. E. *Mol. Phys.* **1986**, *58*, 401.
- (35) Fan, K.; Xie, Y.; Boggs, J. E. *THEOCHEM* **1986**, *136*, 339.
- (36) Lee, S. Y.; Boo, B. H. *J. Phys. Chem.* **1996**, *100*, 15073–15078.
- (37) Majoube, M.; Vergoten, G. *J. Raman Spectrosc.* **1992**, *23*, 431.
- (38) Devlin, F. J.; Finley, J. W.; Stephens, P. J.; Frisch, M. J. *J. Phys. Chem.* **1995**, *99*, 16883.
- (39) Handy, N. C.; Murray, C. W.; Amos, R. D. *J. Phys. Chem.* **1993**, *97*, 4392.
- (40) El-Azhary, A. A.; Suter, H. U. *J. Phys. Chem.* **1995**, *99*, 12751.
- (41) Wheelless, C. J. M.; Zhou, X.; Liu, R. *J. Phys. Chem.* **1995**, *99*, 12488.
- (42) Rauhut, G.; Pulay, P. *J. Phys. Chem.* **1995**, *99*, 3093.
- (43) Johnson, B. G.; Gill, P. M. W.; Pople, J. A. *J. Chem. Phys.* **1993**, *98*, 5612.
- (44) Langhoff, S. R. *J. Phys. Chem.* **1996**, *100*, 2819.
- (45) *HyperChem Ver. 6.01 Molecular Modeling System runs under MS-Windows*; HyperCube Inc.: Gainesville, FL, 2000.
- (46) The FreqChk utility under GAUSSIAN 98W has two distinct modes of operation: (a) retrieving frequencies and thermodynamics data from a checkpoint file or (b) preparing a molecular modeling file and a script file for HyperChem program to visualize and animate the computed normal vibrational modes.
- (47) Gerdil, R. *Acta Crystallogr.* **1961**, *14*, 333.
- (48) Jeffrey, G. A.; Ruble, J. R.; Yates, J. H. *Acta Crystallogr.* **1983**, *B39*, 388.
- (49) Ferenczy, G.; Harsanyi, L.; Rozasondai, B.; Hargittai, I. *J. Mol. Struct.* **1986**, *140*, 71.